Biomech Model Mechanobiol (2012) 11:1097–1108
DOI 10.1007/s10237-012-0376-9

ORIGINAL PAPER

A multiscale approach to the elastic moduli of biomembrane networks

F. Fraternali · G. Marcelli

Received: 8 September 2011 / Accepted: 18 January 2012 / Published online: 17 February 2012

Abstract We develop equilibrium fluctuation formulae for the isothermal elastic moduli of discrete biomembrane models at different scales. We account for the coupling of large stretching and bending strains of triangulated network models endowed with harmonic and dihedral angle potentials, on the basis of the discrete-continuum approach presented in Schmidt and Fraternali (J Mech Phys Solids 60:172–180, 2012). We test the proposed equilibrium fluctuation formulae with reference to a coarse-grained molecular dynamics model of the red blood cell (RBC) membrane (Marcelli et al. in Biophys J 89:2473–2480, 2005; Hale et al. in Soft Matter 5:3603–3606, 2009), employing a local maximum-entropy regularization of the fluctuating configurations (Fraternali et al. in J Comput Phys 231:528–540, 2012). We obtain information about membrane stiffening/softening due to stretching, curvature, and microscopic undulations of the RBC model. We detect local dependence of the elastic moduli over the RBC membrane, establishing comparisons between the present theory and different approaches available in the literature.

Keywords Biomembranes · Bending · Stretching · Thermal fluctuations · Red blood cell model

F. Fraternali (✉)
Department of Civil Engineering, University of Salerno,
84084 Fisciano, SA, Italy
e-mail: fernando.fraternali@kcl.ac.uk

F. Fraternali
Division of Engineering, King's College London, Strand,
London WC2R 2LS, UK

G. Marcelli
School of Engineering and Digital Arts, University of Kent,
Jennison Building, Canterbury, Kent CT2 7NT, UK
e-mail: g.marcelli@kent.ac.uk

1 Introduction

The estimation of the limiting elastic properties of discrete network models of plates and shells is a key feature of atomistic approaches to the mechanics of 2D continua, bio- and nano-structures (refer e.g., to Nelson et al. (2004), Müller et al. (2006), Schmidt (2006), Schmidt (2008), Tu and Ou-Yang (2008), Hartmann (2010) and references therein). In the case of triangular nets, well-established results have been found for the stretching moduli (area compression modulus and in-plane shear modulus in the isotropic case), considering both infinitesimal and large membrane deformations (Seung and Nelson 1988; Discher et al. 1997; Zhou and Joós 1997). More puzzling is the determination of the bending moduli of triangulated surface networks, especially when cosine-type dihedral angle potentials are employed, since shape-dependent estimates have been proposed in the literature for such networks (Nelson et al. 2004; Gompper and Kroll 1996). Universal formulae for the limiting stretching and bending energies of membrane networks have been recently formulated in Schmidt and Fraternali (2012), accounting for the coupling of stretching and bending strains in the finite elasticity regime.

The effects of thermal fluctuations (or undulations) on the elastic rigidities of flexible membranes have been extensively investigated in the literature through different approaches (refer e.g., to Zhou and Joós (1997), Gompper and Kroll (1996), Lee and Discher (2001), Helfrich and Servuss (1984), Helfrich (1985, 1998), Pinnow and Helfrich (2000) and references therein). Zhou and Joós (1997) applied an equilibrium fluctuation (EF) approach to quantify Lamé constants, used as stability criteria for membrane fracture. The EF approach is particularly convenient in practical applications, since it calculates the elastic constants from the microscopic fluctuations of the system during a single run of a Molecular

Dynamics (MD) simulation (Zhou and Joós 1999) and often leads to fast convergence of the estimates (Yoshimoto et al. 2005). It is based on taking the second derivatives of an appropriate free energy (the Helmholtz free energy in the case of a canonical ensemble) with respect to macroscopic strain measures, in correspondence with the fluctuating configurations of the system. EF formulae for the elastic constants distinguish different contributions to the overall moduli [Born, fluctuation, stress and kinetic terms, according to the notation used in Zhou and Joós (2002)]. It can be shown that the fluctuation terms of the Lamé constants of flat membranes are always negative (Zhou and Joós 1997, 1999), which implies softening of the elastic response due to microscopic fluctuations. We refer the reader to Squire et al. (1969), Ray and Rahman (1984), Lutsko (1989), Zhou and Joós (1996, 1997, 1999, 2002), Hess et al. (1997), Schöffel and Möser (2001), Yoshimoto et al. (2005) and references therein for more details about the EF approach. An alternative approach has been proposed in Lee and Discher (2001) for the shear and bulk moduli of 2D fluctuating networks, making use of the equipartition theorem of statistical mechanics. For what concerns the bending modulus, several approaches based on the equipartition theorem and renormalization methods have been proposed in the literature (Peliti and Leibler 1985; Kleinert 1986; Gompper and Kroll 1996; Helfrich and Servuss 1984; Helfrich 1985, 1998; Pinnow and Helfrich 2000). Different approaches have led to contradictory results in terms of the nature of fluctuation effects on the bending response. Some pioneeristic works predicted membrane softening due to thermal undulations (Helfrich 1985; Peliti and Leibler 1985; Kleinert 1986). Such results were later on confirmed by Monte Carlo simulations by Gompper and Kroll (1996). Subsequently, Helfrich and coworkers instead observed membrane stiffening by thermal undulations (Helfrich 1998; Pinnow and Helfrich 2000), through a suitable correction of the approach proposed in Helfrich (1985). Recent results by Kohyama (2009) again predict that thermal fluctuations soften the bending response of coarse-grained models of flexible membranes.

In this work, we develop an equilibrium fluctuation approach to derive the elastic moduli of membrane networks undergoing large stretching and bending deformations. We generalize the discrete to continuum approach presented in Schmidt and Fraternali (2012) to perform differentiation of the Helmholtz free energy with respect to continuum strain measures of the fluctuating surface. The latter are estimated through the local maximum-entropy (LME) regularization proposed in Fraternali et al. (2012). We develop equilibrium fluctuation formulae for the entire set of isothermal (stretching-bending) elastic moduli. The proposed formulae are tested with reference to a discrete model of the red blood cell (RBC) membrane (Marcelli et al. 2005; Hale et al. 2009), providing spatial distributions and global statistics of the shear and bending moduli of such a model. We establish comparisons between the predictions of the present approach and those given in Lee and Discher (2001), Peliti and Leibler (1985), Kleinert (1986), Gompper and Kroll (1996), Helfrich and Servuss (1984), Helfrich (1985, 1998), Helfrich and Kozlov (1993), Pinnow and Helfrich (2000). It is worth noting that the bending–stretching coupling effects covered by the present analysis are not accounted for in standard approaches to the combined stretching–bending response of membrane networks [refer e.g., to Lipowski and Girardet (1990)]. We investigate on the isothermal elastic moduli of fluctuating membranes through an original equilibrium fluctuation approach, which in particular accounts for variable curvature and stretching strains over the simulation patch. The numerical results presented in this work highlight RBC membrane stiffening due to local area contraction and curvature of the network, and softening due to area expansion and thermal fluctuations. Such effects vary from point to point, introducing a topological variability of the referential moduli at the mesocopic scale, which can be usefully exploited to develop continuous modeling informed by MD simulations (information-passing multiscale approach).

The paper is organized as follows. We start by deriving the elastic moduli of static membrane networks in Sect. 2. Next, in Sect. 3, we formulate equilibrium fluctuation formulae for the isothermal moduli of such systems. In Sect. 4, we present a numerical study on the stretching and bending moduli of the RBC membrane. We end by summarizing the main conclusions of the present study and future research directions in Sect. 5.

2 Elastic moduli of static networks

Let us consider a scalar $r_0 > 0$, and a 2D triangular lattice $\mathcal{L}$ with lattice vectors of components

$$\mathbf{a}_1 = \begin{pmatrix} -r_0/2 \\ \sqrt{3}r_0/2 \end{pmatrix}, \quad \mathbf{a}_2 = \begin{pmatrix} -r_0/2 \\ -\sqrt{3}r_0/2 \end{pmatrix}, \quad \mathbf{a}_3 = \begin{pmatrix} r_0 \\ 0 \end{pmatrix},$$

with respect to a Cartesian frame $\{\mathbf{e}_1, \mathbf{e}_2\}$ having $\mathbf{e}_1$ aligned with $\mathbf{a}_3$. A finite piece of such a lattice, showing N nodes or particles, is given by $\mathcal{L}_N = \mathcal{L} \cap U$, where U is a bounded open subset of $\mathbb{R}^2$. We assume that $\mathcal{L}_N$ represents the reference configuration of a membrane network X_N lying in the 3D Cartesian space. We also assume that the deformed configuration of X_N is defined by the restriction of a continuous deformation mapping $f : U \to \mathbb{R}^3$ to $\mathcal{L}_N$. The potential energy of X_N is supposed to have the following expression

$$E_r(f) = E_r^{\text{stretch}}(f) + E_r^{\text{bend}}(f) \tag{1}$$

where

$$E_r^{\text{stretch}}(f) = \frac{k}{2} \sum_{\substack{u,v\in\mathcal{L}_r\cap U \\ |u-v|=r}} (|f(u)-f(v)|-r_0)^2 \tag{2}$$

$$E_r^{\text{bend}}(f) = \frac{D}{2} \sum_{\substack{\triangle,\triangle'\in\mathcal{C}_r \\ \text{neighbors}}} |n_\triangle - n_{\triangle'}|^2 \tag{3}$$

are energies corresponding to nearest-neigbor linear bonds and dihedral angle potentials, respectively. In (2), (3), k is a linear spring stiffness parameter; D is an angular spring stiffness parameter; $\mathcal{C}_r$ is the set of equilateral triangles $\triangle \subset U$ with sidelength r_0 and vertices in $\mathcal{L}_r$; and $n_\triangle$ is the unit normal to $f(n_\triangle)$.

Let $\mathbf{I}(u) = (g_{ij})$ and $\mathbf{II}(u) = (h_{ij})$ denote the first and second fundamental forms of the 3D surface S mapped by $f(u)$, which are given by [refer, e.g., to Kühnel (2002)]

$$g_{\alpha\beta} = \mathbf{g}_\alpha \cdot \mathbf{g}_\beta, \quad h_{\alpha\beta} = \mathbf{n} \cdot \mathbf{g}_{\alpha,\beta} \tag{4}$$

where

$$\mathbf{g}_\alpha = \sum_{i=1}^{3} f_{i,\alpha}\hat{\mathbf{e}}_i, \quad \mathbf{n} = \frac{\mathbf{g}_1 \times \mathbf{g}_2}{|\mathbf{g}_1 \times \mathbf{g}_2|} \tag{5}$$

It has been shown in Schmidt and Fraternali (2012) that the continuum limit $r_0 \to 0$ ($N \to \infty$) of the discrete energy (1) is the following

$$E(f) := \lim_{r_0\to 0} E_r(f) = \int_U (W^{\text{bend}}(\mathbf{I}(u), \mathbf{II}(u)) + W^{\text{stretch}}(\mathbf{I}(u)))\, \mathrm{d}u \tag{6}$$

where

$$\begin{aligned} &W^{\text{bend}}(\mathbf{I}(u), \mathbf{II}(u)) \\ &= \frac{\sqrt{3}D}{12\det\mathbf{I}} \left(g_{11}(h_{11}^2 + 2h_{12}^2 - 2h_{11}h_{22} + 3h_{22}^2\right) \\ &\quad -8g_{12}h_{11}h_{12} + 2g_{22}(h_{11}^2 + 3h_{12}^2)) \end{aligned} \tag{7}$$

$$W^{\text{stretch}}(\mathbf{I}(u)) = \frac{k}{\sqrt{3}} \sum_{i=1}^{3} (\lambda_i(\mathbf{I}(u)) - 1)^2 \tag{8}$$

with

$$\begin{aligned} \lambda_1 &= \frac{1}{2}\sqrt{g_{11} - 2\sqrt{3}g_{12} + 3g_{22}} \\ \lambda_2 &= \frac{1}{2}\sqrt{g_{11} + 2\sqrt{3}g_{12} + 3g_{22}} \\ \lambda_3 &= \sqrt{g_{11}} \end{aligned} \tag{9}$$

We now introduce the total limiting energy density

$$W^{\text{limit}}(\mathbf{I}(u), \mathbf{II}(u)) = W^{\text{stretch}}(\mathbf{I}(u)) + W^{\text{bend}}(\mathbf{I}(u), \mathbf{II}(u)) \tag{10}$$

and the numerical vectors $\mathbf{g} = (g_{11}, g_{22}, 2g_{12})$ and $\mathbf{h} = (h_{11}, h_{22}, 2h_{12})$, which collect the independent components of the symmetric tensors $\mathbf{I}$ and $\mathbf{II}$, respectively. By differentiating W^{limit} with respect to $\mathbf{g}$ and $\mathbf{h}$, we get the following expressions the referential stretching stresses $\mathbf{N} = (N_i)$; bending stresses $\mathbf{M} = (M_i)$; stretching moduli $\mathbf{A} = (A_{ij})$; bending moduli $\mathbf{D} = (D_{ij})$; and bending–stretching moduli $\mathbf{B} = (B_{ij})(i, j = 1, 2.3)$ of X_N

$$\mathbf{N} = 2\frac{\partial W^{\text{limit}}}{\partial \mathbf{g}}, \quad \mathbf{M} = \frac{\partial W^{\text{limit}}}{\partial \mathbf{h}} \tag{11}$$

$$\mathbf{A} = 4\frac{\partial^2 W^{\text{limit}}}{\partial \mathbf{g}^2}, \quad \mathbf{B} = 2\frac{\partial^2 W^{\text{limit}}}{\partial \mathbf{g}\partial \mathbf{h}}, \quad \mathbf{D} = \frac{\partial^2 W^{\text{limit}}}{\partial \mathbf{h}^2} \tag{12}$$

For convenience, we group the above quantities into the following arrays

$$\mathbf{S} = \begin{bmatrix} \mathbf{N} \\ \mathbf{M} \end{bmatrix}, \ \mathbf{Q} = \begin{bmatrix} \mathbf{e} \\ \mathbf{h} \end{bmatrix}, \ \mathbf{C} = \left[\begin{array}{c|c} \mathbf{A} & \mathbf{B} \\ \hline \mathbf{B}^T & \mathbf{D} \end{array}\right] \tag{13}$$

which define the overall (stretching-bending) stress vector, strain vector, and elasticity matrix of the network, with $\mathbf{e} = \frac{1}{2}(g_{11} - 1, g_{22} - 1, 2g_{12})$. We refer the reader to Schmidt and Fraternali (2012) for the detailed expressions of the quantities appearing on the r.h.s of $(13)_1$, $(13)_3$, which depend on both the stretching strains (g_{ij}) and the bending strains (h_{ij}) of S (Naghdi 1972). The innovative character of the present approach, as compared to standard models of flexible membranes, follows from the expression (7) of the limiting bending energy. Such an energy indeed accounts for a 'multiplicative' composition of stretching and bending strains, while standard energy models instead feature terms that alternatively include either stretching or bending strains [refer, e.g., to Lipowski and Girardet (1990)]. For later use, we introduce the following quantities

$$\begin{aligned} \mu^1 = C_{33} &= \frac{\sqrt{3}k}{\left(g_{11} + 2\sqrt{3}g_{12} + 3g_{22}\right)^{3/2}} \\ &\quad + \frac{\sqrt{3}k}{\left(g_{11} - 2\sqrt{3}g_{12} + 3g_{22}\right)^{3/2}} \\ &\quad + \frac{D}{2\sqrt{3}(\det\mathbf{I})^3}\,(-16g_{12}(\det\mathbf{I})h_{11}h_{12} \\ &\quad - \left(g_{11}g_{22} + 3g_{12}^2\right) \\ &\quad \times \left(8g_{12}h_{11}h_{12} - 2g_{22}\left(h_{11}^2 + 3h_{12}^2\right)\right. \\ &\quad \left. -g_{11}\left(h_{11}^2 - 2h_{11}h_{22} + 2h_{12}^2 + 3h_{22}^2\right)\right)\right) \end{aligned} \tag{14}$$

$$\kappa_H^1 = \frac{C_{44} + 2C_{45} + C_{55} + C_{66}}{4} = \frac{\sqrt{3}D\,(g_{11}+2g_{22})}{6\det\mathbf{I}} \tag{15}$$

which define static shear and bending stiffness measures accounting for large stretching and bending deformations of the reference lattice, respectively (Schmidt and Fraternali

2012). It is not difficult to realize that the above quantities assume the following simplified expressions

$$\mu^1 \approx \mu^0 = \frac{\sqrt{3}k}{4}, \quad \kappa_H^1 \approx \kappa_H^0 = \frac{\sqrt{3}D}{2} \tag{16}$$

in the infinitesimal elasticity regime [$\mathbf{I}$ approximatively coincident with the identity matrix; $D|\mathbf{II}|^2 \ll k$, cf. also Schmidt and Fraternali (2012)].

3 Isothermal elastic moduli of fluctuating networks

Let us consider a portion (or 'patch') $X_{N'}$ of X_N, which is composed of $N' \leq N$ particles. From now on we assume that X_N fluctuates at constant absolute temperature T in the 3D Cartesian space (Fig. 1). We initially consider the elastic moduli of $X_{N'}$ in the stress-free reference configuration and neglect kinetic terms (refer, e.g., to Zhou and Joós (1996, 2002), Schöffel and Möser (2001) for the different terms of EF formulas). We thus introduce the Helmholtz free energy

$$F' = -k_B T \log Z' \tag{17}$$

where Z' is the partition function given by

$$Z' = \int \mathrm{e}^{-E_r/k_B T} \, \mathrm{d}\mathbf{r} \tag{18}$$

In (18), k_B is the Boltzmann constant, and $\mathbf{r}$ denotes the position vector. A discrete to continumm approach to the elastic response of $X_{N'}$ is obtained by introducing the following continuum regularization of E_r

$$E_r \approx \sum_{a=1}^{N'} W^a A_0^a \tag{19}$$

into (18). Such a regularization is defined over a 'dual' tessellation (or mesh) $\{\sigma^1, \ldots, \sigma^{N'}\}$ of the reference lattice (Munkres 1984), which we assume composed of polygons joining the barycenters of the reference triangles (barycentric dual mesh, cf. Fig. 1). We use the symbol A_0^a to denote the surface area of σ^a, and W^a to denote the quantity $W^{\text{limit}}(\mathbf{I}^a, \mathbf{II}^a)$, where $\mathbf{I}^a$ and $\mathbf{II}^a$ are suitable estimates of the first and second fundamental forms of the current configuration of σ^a (obtained, e.g., through the Local Maximum-Entropy regularization scheme presented in Fraternali et al. (2012), which is briefly sketched in the "Appendix" to the present paper).

We estimate the referential elasticity tensor $\hat{\mathbf{C}}' = (\hat{C}'_{ij})$ of $X_{N'}$ through the following *equilibrium fluctuation formulae*:

$$\hat{C}'_{ij} = \frac{1}{A_0} \sum_{a=1}^{N'} \frac{\partial^2 F'}{\partial Q_i^a \partial Q_j^a} \quad (i, j = 1, \ldots, 6) \tag{20}$$

where A_0 denotes the total surface area of $X_{N'}$ in the reference configuration, and Q_{ij}^a denotes the strain vector associated with $\mathbf{I}^a$ and $\mathbf{II}^a$ through (13). It is worth noting that

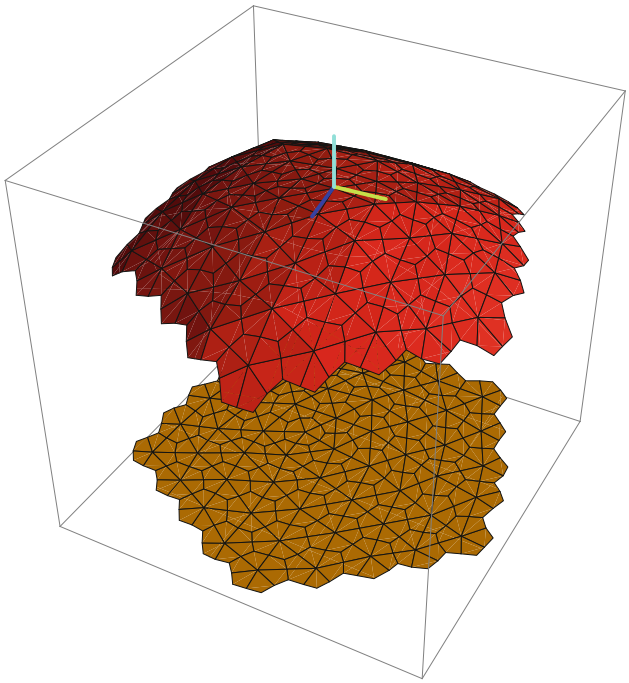

Fig. 1 Reference (flat) and current configurations of a portion $X_{N'}$ of a fluctuating network X_N

Eq. (20) accounts for variable strains measures Q_i^a from cell to cell of $X_{N'}$ (e.g., variable curvatures associated with out-of-plane displacements, cf. Fig. 1) and homogeneous strains over each single cell. We also wish to remark that the present fixed-reference (or material) approach to the elastic moduli of $X_{N'}$ (cf. Ogden (1984), Sect. 6.1.3; Holzapfel (2000), Sect. 6.6) accounts for arbitrarily large deformations from the reference configuration. A straightforward calculation gives

$$\frac{\partial^2 F'}{\partial Q_i^a \partial Q_j^a} = \left\langle \frac{\partial^2 E_r}{\partial Q_i^a \partial Q_j^a} \right\rangle - \frac{1}{k_B T} \left(\left\langle \frac{\partial E_r}{\partial Q_i^a} \frac{\partial E_r}{\partial Q_j^a} \right\rangle - \left\langle \frac{\partial E_r}{\partial Q_i^a} \right\rangle \left\langle \frac{\partial E_r}{\partial Q_j^a} \right\rangle \right) \tag{21}$$

where $\langle(\cdot)\rangle$ denotes the configurational average of the quantity $(\cdot)$. On substituting (21) into (20) and accounting for (19), we finally obtain

$$\hat{C}'_{ij} = C_{ij}^B + C_{ij}^F \tag{22}$$

where

$$C_{ij}^B = \frac{1}{A_0} \sum_{a=1}^{N'} \left\langle C_{ij}^a \right\rangle A_0^a \tag{23}$$

$$C_{ij}^F = -\frac{1}{k_B T A_0} \sum_{a=1}^{N'} \left(\left\langle S_i^{B_a} \, S_j^{B_a} \right\rangle - \left\langle S_i^{B_a} \right\rangle \left\langle S_j^{B_a} \right\rangle \right) \left(A_0^a \right)^2 \tag{24}$$

with

$$S_i^{B_a} = \frac{\partial W^a}{\partial Q_i^a}, \quad C_{ij}^a = \frac{\partial^2 W^a}{\partial Q_i^a \partial Q_j^a} \tag{25}$$

The quantities C_{ij}^B and C_{ij}^F define the Born and fluctuation terms of $\hat{C}'_{ij}$, respectively (Zhou and Joós 1996, 2002). The Born terms are computed from the thermal averages of the second derivatives of the limiting strain energy densities of the dual cells and approximate the zero-temperature elastic coefficients of the system (Lutsko 1989), while the fluctuation terms account for the microscopic fluctuations of each $\sigma^a \in X_N$ around the mean shape. Formulae (22)–(25) apply to an arbitrary membrane network model, provided that W^a is properly defined. In the special case of the model introduced in the previous section, it results $A_0^a = A_0/N'$ at every σ^a, and therefore it results

$$C_{ij}^B = \frac{1}{N'} \sum_{a=1}^{N'} \left\langle C_{ij}^a \right\rangle, \quad C_{ij}^F = -\frac{A_0}{(N')^2 k_B T} \sum_{a=1}^{N'} \left(\left\langle S_i^{B_a} \, S_j^{B_a} \right\rangle - \left\langle S_i^{B_a} \right\rangle \left\langle S_j^{B_a} \right\rangle \right) \tag{26}$$

$$S_i^B = \frac{1}{N} \sum_{a=1}^{N'} \left\langle S_i^{B_a} \right\rangle \tag{27}$$

We now compute the total elastic moduli $\hat{C}_{ij}$ of $X_{N'}$, which are derived from the addition of loading and kinetic terms to the free energy of the system, on adopting the notation of Zhou and Joós (1996, 1997, 2002) [notice that sometimes a different nomenclature is encountered in the literature, which incorporates the stress terms of the elastic coefficients into the Born terms, refer e.g., to Hess et al. (1997)]. Supposing that $X_{N'}$ is subject to dominant stretching stresses (as compared to bending stresses), we determine its total moduli by adding the stress and kinetic terms deduced from Zhou and Joós (1996) for a 2D flat membrane to the referential elasticity tensor $\hat{C}'_{ij}$ defined by Eq. (22). We finally write

$$\hat{C}_{ij} = C_{ij}^B + C_{ij}^F + C_{ij}^K + C_{ij}^S \tag{28}$$

where (cf. equations (61), (64) and (65) of Zhou and Joós (1996))

$$\mathbf{C}^K = \left[\begin{array}{c|c} \frac{N' k_B T}{A_0} \begin{pmatrix} 2 & 0 & 0 \\ 0 & 2 & 0 \\ 0 & 0 & 1 \end{pmatrix} & \begin{pmatrix} 0 & 0 & 0 \\ 0 & 0 & 0 \\ 0 & 0 & 0 \end{pmatrix} \\ \hline \begin{pmatrix} 0 & 0 & 0 \\ 0 & 0 & 0 \\ 0 & 0 & 0 \end{pmatrix} & \begin{pmatrix} 0 & 0 & 0 \\ 0 & 0 & 0 \\ 0 & 0 & 0 \end{pmatrix} \end{array} \right] \tag{29}$$

$$\mathbf{C}^S = \left[\begin{array}{ccc|c} \hat{S}_1 & -\frac{1}{2}(\hat{S}_1 + \hat{S}_2) & \frac{1}{2}\hat{S}_3 & \begin{pmatrix} 0 & 0 & 0 \\ 0 & 0 & 0 \\ 0 & 0 & 0 \end{pmatrix} \\ -\frac{1}{2}(\hat{S}_1 + \hat{S}_2) & \hat{S}_2 & \frac{1}{2}\hat{S}_3 & \\ \frac{1}{2}\hat{S}_3 & \frac{1}{2}\hat{S}_3 & \frac{1}{2}(\hat{S}_1 + \hat{S}_2) & \\ \hline \begin{pmatrix} 0 & 0 & 0 \\ 0 & 0 & 0 \\ 0 & 0 & 0 \end{pmatrix} & & & \begin{pmatrix} 0 & 0 & 0 \\ 0 & 0 & 0 \\ 0 & 0 & 0 \end{pmatrix} \end{array} \right] \tag{30}$$

In (30), it results $\hat{S}_1 = S_1^B - N' k_B T/A_0$, $\hat{S}_2 = S_2^B - N' k_B T/A_0$, $\hat{S}_3 = S_3^B$, with

$$S_i^B = \frac{1}{A_0} \sum_{a=1}^{N'} \left\langle S_i^{B_a} \right\rangle A_0^a \tag{31}$$

The isothermal values of the area compression modulus $\hat{\kappa}_A$, in-plane shear modulus $\hat{G}_{12}$, and bending modulus $\hat{\kappa}_H$ of $X_{N'}$ are given by (Schmidt and Fraternali 2012)

$$\hat{\kappa}_A = \frac{1}{\hat{C}_{11}^{-1} + 2\hat{C}_{12}^{-1} + \hat{C}_{22}^{-1}}, \quad \hat{G}_{12} = \frac{1}{\hat{C}_{33}^{-1}}, \quad \hat{\kappa}_H = \frac{\hat{C}_{44} + 2\hat{C}_{45} + \hat{C}_{55} + 4\hat{C}_{66}}{4} \tag{32}$$

It is not difficult to show that the diagonal elements of the fluctuation elasticity matrix C_{ij}^F are non-positive, which implies membrane softening by thermal fluctuations within the present theory. This is in agreement with the equilibrium fluctuation approach by Zhou and Joós (1996, 1997). It is also possible to show that the fluctuation term of the bending modulus

$$\kappa_H^F = \frac{C_{44}^F + 2C_{45}^F + C_{55}^F + 4C_{66}^F}{4} \tag{33}$$

is non-positive. The corresponding Born term is given by

$$\kappa_H^B = \frac{C_{44}^B + 2C_{45}^B + C_{55}^B + 4C_{66}^B}{4} \tag{34}$$

and it is easy to recognize that such a quantity coincides with the configurational average $\langle \kappa_H^1 \rangle$ of the static bending modulus (15). We note that it is not possible to similarly define Born and fluctuation terms of $\hat{\kappa}_A$ and $\hat{G}_{12}$, since such quantities are obtained by manipulating the inverse of the global elasticity matrix (cf. Eq. $(32)_{1,2}$), which mixes up all the different contributions to $\hat{C}_{ij}$.

4 Numerical results and discussion

We test the equilibrium fluctuation formulae developed in the previous section with reference to the coarse-grained MD model of the red blood cell membrane presented in Marcelli et al. (2005) and Hale et al. (2009). Such a model describes the RBC wall as a triangulated membrane network X_N composed of N particles and of $M = 2N - 4$ triangles. The side length r_0 of the primal triangles is set equal to the average length of the spectrin filaments (∼100 nm) forming the

cytoskeleton of a real RBC cell in normal conditions (Hale et al. 2009). The model is equipped with bond and dihedral angle potentials described by Eqs. (2) and (3), respectively. It includes an area constraints requiring that the global surface area ($A_{\rm tot}$) of the membrane remains constantly equal to that characterizing the reference configuration (Marcelli et al. 2005), and a volume constraint requiring that the volume enclosed by the membrane ($V_{\rm tot}$) is constantly equal to 0.65 times the volume of a sphere with the same surface area (Hale et al. 2009). Isothermal fluctuations of the RBC membrane are simulated through the MD software DLPOLY version 2.20 developed in Daresbury Laboratory, Cheshire, UK (Smith and Forester 1999), employing the Nosé–Hoover thermostat to keep the temperature constant; 3×10^6 steps with time-step $\Delta t = 2.07 \times 10^{-5}\ t_0$, where $t_0 = \sqrt{m/k}$; $N = 5762$ particles; particle mass $m = 5.82625 \times 10^{-20}$ kg; $k = 8.3\,\mu$N/m; $D = 130 \times 10^{-20}$ J; absolute temperature $T = 309$ K; $A_{\rm tot} = 4.986 \times 10^7$ nm^2; $V_{\rm tot} = 3.311 \times 10^{10}$ nm^3. The initial configuration is chosen to be the icosahedron such that each particle shows equal distance r_0 from all the nearest neighbors. The cell model is treated as an isolated systems, in contact with an artificial thermal bath, so no boundary conditions are applied. The instantaneous cell volume is computed as the sum of the volumes of pyramids sharing a point placed in the interior of the cell as vertex and featuring the current configurations of the mesh triangles as bases. It has been observed in Hale et al. (2009) that the adopted material constants k and D, in association with the volume and area constraints, drive the cell model to acquire on average a discoid shape, reproducing experimentally observed mean square fluctuations of the equatorial contours of real RBC cells.

In correspondence with each individual particle $\mathbf{x}_a$ of X_N, we consider a patch $X^a_{N'} \subset X_N$ formed by the mth order nearest neighbors of $\mathbf{x}_a$ (cf. Fig. 1, where $m = 5$), in order to obtain mesoscopic estimates of the elastic moduli of the RBC membrane, for different choices of m. Such estimates are obtained through the equilibrium fluctuation formulae (22)–(24), employing LME approximations of the first and second fundamental forms of the deformed cells σ^a (Fraternali et al. 2012), at each step of the MD simulation (cf. the "Appendix").

We focus our attention on the isothermal values $(32)_{2,3}$ of the in-plane shear modulus $\hat{G}_{12}$ and bending modulus $\hat{\kappa}_H$ of the RBC model, observing that its 'macroscopic' area compression modulus is infinitely large, due to the global area constraint. We also investigate on the Born, fluctuation, stress and kinetic terms of the 'isotropic' shear modulus $\hat{\mu} \equiv \hat{C}_{33}$, and the Born and fluctuation terms of bending modulus $\hat{\kappa}_H$ (the latter exhibits zero stress and kinetic terms, cf. Sect. 3).

It is not difficult to show that $\mu^1 \equiv C_{33}$ approximate the in-plane shear modulus $G_{12} \equiv 1/C^{-1}_{33}$ of a static network in the infinitesimal elasticity regime, where the limiting elastic response of the current network model is actually isotropic (Schmidt and Fraternali 2012). The shear moduli μ and G_{12} may instead significantly differ from each other in the large strain regime, where the use of G_{12} allows one to account for the material anisotropy arising in the continuum limit (Schmidt and Fraternali 2012). We include $\hat{\mu}$ in our analysis in order to investigate on the different contributions to the shear rigidity of the network, which are not additively separable in $\hat{G}_{12}$ (cf. Sect. 3), and also to establish comparisons with the equipartition analysis presented in Lee and Discher (2001). In the following, we will refer to $\hat{G}_{12}$ as the 'anisotropic' shear modulus of the network.

We look at the ratios between the examined moduli and the 'stress-free' shear and bending moduli of the reference lattice in the infinitesimal elasticity regime, which are given by μ^0 and κ^0_H, respectively (Sect. 2). We say the the membrane is undergoing *softening* of the shearing (bending) response when the $\hat{G}_{12}/\mu^0$ ($\hat{\kappa}_H/\kappa^0_H$) ratio is less than unity, and shearing (bending) *stiffening* when the same ratio is instead greater than one.

It is useful to observe that the Born terms $\mu^B \equiv \langle \mu^1 \rangle$ and $\kappa^B_H \equiv \langle \kappa^1_H \rangle$ of $\hat{\mu}$ and $\hat{\kappa}_H$ estimate the isotropic shear modulus and the bending modulus at zero temperature in the finite elasticity regime, respectively (Lutsko 1989).

4.1 Average strain and fluctuation measures

The following analysis deals with average strain and fluctuation measures of the RBC model. Regarding average strains, we analyze the area stretching ratio $\sqrt{\langle g \rangle} = \sqrt{\langle \det \mathbf{I} \rangle}$; the shear strain $\langle g_{12} \rangle$; the mean curvature $\langle H/2 \rangle$; and the Gaussian curvature $\langle K \rangle$ of the mean shape. The examined fluctuation measures instead consist of the quantities $\langle u^2_\parallel \rangle$ and $\langle u^2_\perp \rangle$, where

$$u_\parallel = \sqrt{\left((\mathbf{x}_a - \langle \mathbf{x}_a \rangle) \cdot \mathbf{k}^a_1\right)^2 + \left((\mathbf{x}_a - \langle \mathbf{x}_a \rangle) \cdot \mathbf{k}^a_2\right)^2}, \tag{35}$$

$$u_\perp = (\mathbf{x}_n - \langle \mathbf{x}_n \rangle) \cdot \mathbf{k}^a_3 \tag{36}$$

Here, $\mathbf{k}^a_1$ and $\mathbf{k}^a_2$ denote the unit tangents to the lines of curvature of the mean shape, which are computed through the LME approach presented in "Appendix" [cf. also Fraternali et al. (2012)].

Table 1 shows the global statistics of the effective strain and fluctuation measures over the RBC membrane, including the mean, standard deviation (SD), minimum and maximum values, and average values over the dimple and rim regions of the membrane. A 3D graphical representation of such quantities is provided by the density plots of Figs. 2 and 3. We note that the area stretching ratio $\sqrt{\langle g \rangle}$ almost symmetrically oscillates around one over the membrane, with -27%, $+20\%$ local oscillations. Local area expansions ($\sqrt{\langle g \rangle} > 1$) are observed at the cell rim, while local area contractions ($\sqrt{\langle g \rangle} < 1$) are observed at the dimple (cf. Fig. 2),

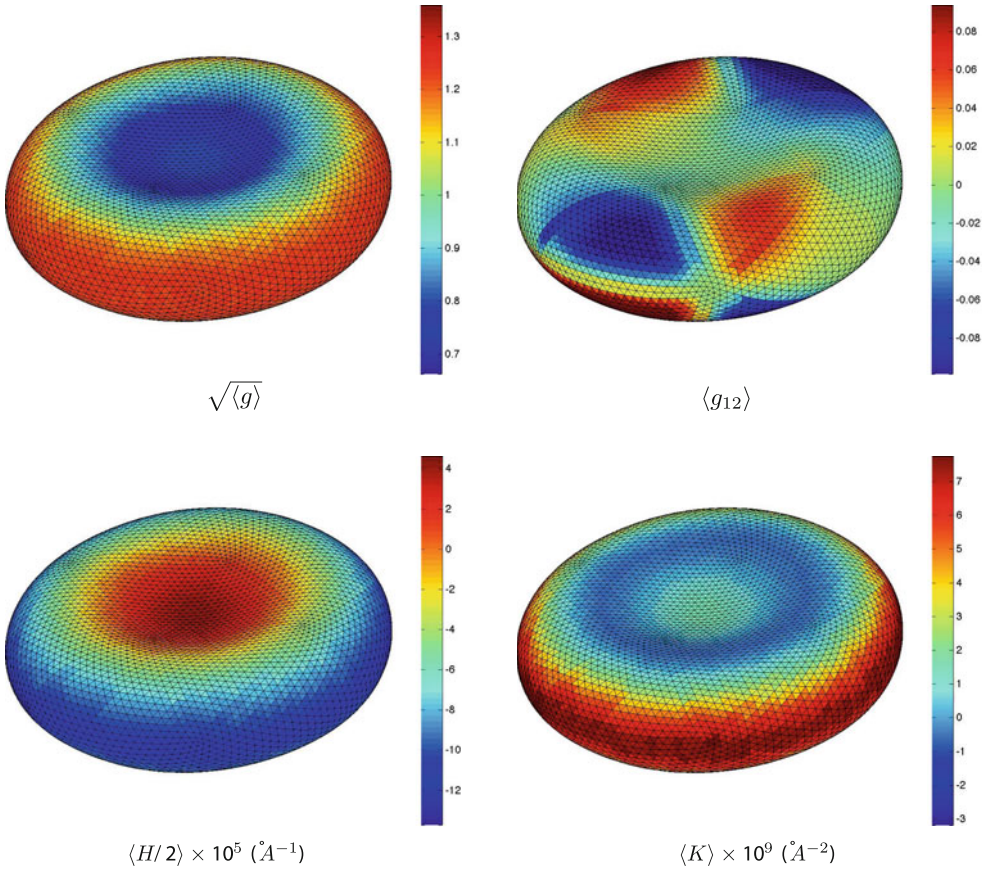

Fig. 2 3D density plots of configurational averages of selected strain measures for isothermal fluctuations ($T = 309$ K) of a CGMD model of the RBC membrane (Marcelli et al. 2005; Hale et al. 2009)

Table 1 Global estimates of effective strain measures, pressure values and fluctuation displacements for isothermal fluctuations ($T = 309$ K) of a CGMD model of the RBC membrane (Marcelli et al. 2005; Hale et al. 2009)

Property	Mean (SD)	Min ÷ max	Dimple ÷ rim
$\sqrt{\langle g \rangle}$	0.98 (0.17)	0.73 ÷ 1.20	0.78 ÷ 1.20
$\langle g_{12} \rangle$	0.00 (0.04)	−0.12 ÷ 0.12	≈0.00 ÷ ±0.12
$\langle H/2 \rangle \times 10^5 (\mathring{A}^{-1})$	−4.56 (4.58)	−10.85 ÷ 3.83	3.83 ÷ −10.74
$\langle K \rangle \times 10^9 (\mathring{A}^{-2})$	2.27 (2.73)	−0.47 ÷ 7.57	1.47 ÷ 7.42
p^B/μ^0	0.16 (0.25)	−0.12 ÷ 0.60	0.52 ÷ −0.12
$\hat{p}/\mu^0$	0.30 (0.24)	0.03 ÷ 0.69	0.67 ÷ 0.03
$\sqrt{\langle u_\parallel^2 \rangle}/r_0$	0.63 (0.20)	0.30 ÷ 0.88	0.34 ÷ 0.30
$\sqrt{\langle u_\perp^2 \rangle}/r_0$	0.17 (0.01)	0.15 ÷ 0.20	0.15 ÷ 0.19

as a consequence of the combined action of area and volume constraints. Concerning the shear strain $\langle g_{12} \rangle$, we observe from Table 1 and Fig. 2 that such a quantity oscillates around zero over the membrane, with oscillations in the range ±12%. The mean curvature $\langle H/2 \rangle$ alternates positive (around the cell dimple) and negative (rim) values, which correspond to concave and convex regions, respectively. Differently, the Gaussian curvature is positive both at the dimple and the rim, with largest values at the rim, and exhibits negative values over the saddle-shaped dimple–rim transition region [cf. also Fraternali et al. (2012)]. The mean shape of the examined model is dyscotic, as we already observed (Hale et al. 2009). The described 'mean' deformation regime leads to positive values of the in-plane Born pressure $p^B = -(S_1^B + S_2^B)/2$ at the dimple and negative values of the same quantity at the rim. Regarding the total in-plane pressure $\hat{p} = -(\hat{S}_1 + \hat{S}_2)/2$ (including kinetic terms, cf. the previous section), we observe positive values at the dimple,

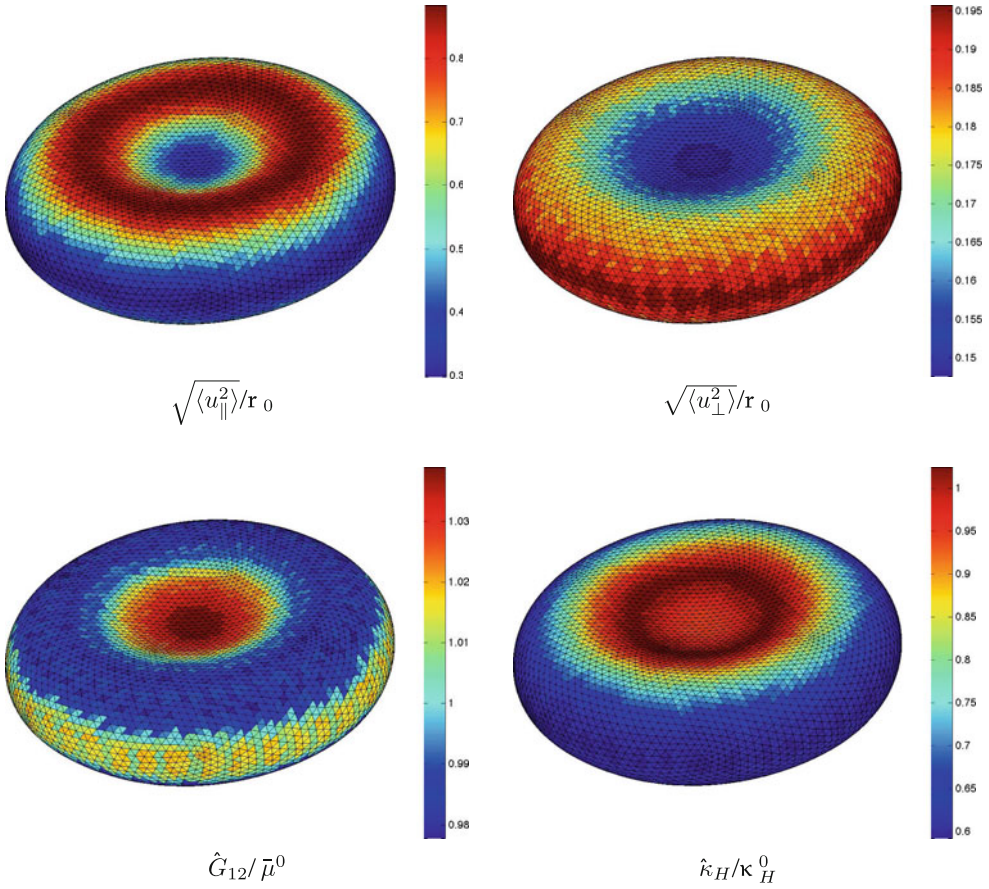

Fig. 3 3D dimensionless density plots of the configurational averages of fluctuation displacements $u_{\parallel}^2$ and $u_{\perp}^2$ from the mean configuration; isothermal shear modulus $\hat{G}_{12}$; and isothermal bending modulus $\hat{\kappa}_H$ ($T = 309\,\mathrm{K}$) for a CGMD model of the RBC membrane (Marcelli et al. 2005; Hale et al. 2009)

and values close to zero at the rim (cf. Table 1, where we report statistics for $N' = 1$). For what regards the fluctuation measures, we observe that the in-plane mean-squared displacement $\langle u_{\parallel}^2 \rangle$ shows the largest values over the dimple–rim transition region, while the out-of-plane mean-squared displacement $\langle u_{\perp}^2 \rangle$ peaks at the rim (Fig. 3). We also notice that $\langle u_{\parallel}^2 \rangle$ exhibits much larger standard deviation than $\langle u_{\perp}^2 \rangle$ (Table 1).

4.2 Elastic moduli

Let us now now examine the spatial distributions and statistics of the shear and bending moduli of the RBC model on hand (Fig. 3; Tables 2 and 3). We consider 'mesoscopic' estimates corresponding to $N' = 19 (m' = 2)$, $N' = 61$ ($m' = 4$), and $N' = 91 (m' = 5)$; and 'macroscopic' estimates corresponding to $N' = N = 5762$ (global effective moduli).

We observe that the mesoscopic estimates of all the examined moduli are stable with the patch size (cf. Tables 2 and 3). Nevertheless, such quantities appreciably oscillate over the membrane, showing noticeable local deviations from the corresponding macroscopic values. Particularly wide oscillations are exhibited by the mesoscopic distributions of the Born term μ^B ($-17\% \div +34\%$ over the macroscopic value) and the isothermal bending modulus $\hat{\kappa}_H$ ($\approx \pm 20\%$ deviations from the macroscopic value, which is in turn 20% smaller than κ_H^0). The anisotropic shear modulus $\hat{G}_{12}$ instead features small oscillations at the mesoscopic scale.

It is useful to look at the deviations between the computed 'static' (μ^B, κ_H^B) and 'dynamic' ($\hat{\mu}, \hat{G}_{12}, \hat{\kappa}_H$) moduli, and the characteristic values μ^0 and κ_H^0. From an analysis of the results in Tables 2 and 3, one realizes that the Born term of the isotropic shear modulus (μ^B) is markedly higher than μ^0 all over the membrane. Such stiffening effects are associated with marked area contraction at the dimple (+66%) and membrane curvature at the rim (+15%). In order to assess the accuracy of the above predictions, we make use of an analytical approximation μ^1 to μ^B, which is obtained on considering Eq. (14), and assuming $g_{11} \approx g_{22} \approx \sqrt{\langle g \rangle}$; $g_{12} \approx 0$ (isotropic membrane stretching); $h_{11}, h_{22} \approx 1/2(\langle H \rangle \pm \sqrt{\langle H \rangle^2 - 4\langle K \rangle})$; $h_{12} \approx 0$ (lines of curvature coincident with the local axes x_1, x_2). The relative approximated version of Eq. (14) gives $\mu^1 \approx \mu^B \approx 1.64\mu^0$ at the dimple (against the computed value $\mu^B = 1.66\mu^0$),

Table 2 Estimates of selected elastic moduli at different scales for isothermal fluctuations ($T = 309\,\mathrm{K}$) of a CGMD model of the RBC membrane (Marcelli et al. 2005; Hale et al. 2009)

	$N' = 19$	$N' = 61$	$N' = 91$	$N' = N = 5762$
μ^B/μ^0	1.15 ÷ 1.66	1.15 ÷ 1.66	1.15 ÷ 1.66	1.32
Dimple ÷ rim	1.66 ÷ 1.15	1.66 ÷ 1.16	1.66 ÷ 1.16	
$\hat{\mu}/\mu^0$	1.01 ÷ 1.15	1.01 ÷ 1.15	1.02 ÷ 1.15	1.08
dimple ÷ rim	1.08 ÷ 1.13	1.08 ÷ 1.14	1.08 ÷ 1.14	
$\hat{G}_{12}/\mu^0$	0.97 ÷ 1.04	0.97 ÷ 1.04	0.98 ÷ 1.04	1.06
dimple ÷ rim	1.04 ÷ 1.00	1.04 ÷ 1.00	1.04 ÷ 1.01	
κ_H^B/κ_H^0	0.83 ÷ 1.29	0.84 ÷ 1.27	0.84 ÷ 1.26	1.02
dimple ÷ rim	1.22 ÷ 0.83	1.23 ÷ 0.84	1.23 ÷ 0.84	
$\hat{\kappa}_H/\kappa_H^0$	0.58 ÷ 1.04	0.59 ÷ 1.03	0.59 ÷ 1.02	0.80
dimple ÷ rim	0.93 ÷ 0.58	0.94 ÷ 0.59	0.94 ÷ 0.59	

The first row of each data section provides minimum and maximum mesoscopic moduli for different choices of N', and effective macroscopic moduli for $N' = N = 5762$. The second row provides average mesoscopic moduli over dimple and rim regions. Reference values for unstressed networks at zero temperature: $\mu^0 = 3.594 \times 10^{-6}\,\mathrm{N/m}$, $\kappa_H^0 = 112.6 \times 10^{-20}\,\mathrm{J}$ ($k = 8.3 \times 10^{-6}\,\mathrm{N/m}$, $D = 130.0 \times 10^{-20}\,\mathrm{J}$)

Table 3 Born, fluctuation and stress terms of $\hat{\mu}/\mu^0$ at the dimple and the rim, for different values of N'

N'	Dimple				Rim			
	Born	Fluct.	Stress	Kin.	Born	Fluct.	Stress	Kin.
19	1.66	−0.06	−0.66	0.14	1.15	−0.13	−0.03	0.14
61	1.66	−0.05	−0.67	0.14	1.16	−0.13	−0.03	0.14
91	1.66	−0.05	−0.67	0.14	1.16	−0.13	−0.03	0.14
5,762	1.32	−0.08	−0.30	0.14	1.32	−0.08	−0.30	0.14

and $\mu^1 \approx \mu^B \approx 1.14\mu^0$ at the rim (which approximatively coincides with the corresponding computed value of μ^B, cf. Table 2). An increase in the shear stiffness of the RBC membrane due to large deformation effects is confirmed by experimental measurements through micropipette aspiration and optical tweezers (cf. Hale et al. (2009) and references therein).

The overall isothermal value of the isotropic shear modulus ($\hat{\mu}$) features 1% ÷ 15% local increases over μ^0, due to the superimposition of stiffening effects due to Born and kinetic terms, and softening effects due to fluctuation and stress terms (Table 3). It is worth noting that the stress term of $\hat{\mu}$ shows opposite sign with respect to the in-plane pressure (cf. Eq. (30) of this paper, and equation (8) of Zhou and Joós (1997)). As we already noticed, the anisotropic shear modulus $\hat{G}_{12}$ instead features small oscillations (−2% ÷ +4%) from μ^0 over the membrane. In particular, the lowest values of $\hat{G}_{12}$ are achieved over the dimple–rim transition region, where the in-plane mean-squared displacement $\langle u_\parallel^2 \rangle$ reaches its maximum (Fig. 3).

Regarding the Born term of the bending modulus (κ_H^B), we observe that this quantity is higher than the corresponding characteristic value κ_H^0 at the dimple (+22%), due to local area contraction, and lower than κ_H^0 at the rim (−17%), due to local area expansion (cf. Table 2). We assess the accuracy of such predictions on employing an analytical approximation κ^1 to κ_H^B, which follows from substituting $g_{11} \approx g_{22} \approx \sqrt{\langle g \rangle}$ and $g_{12} \approx 0$ into the r.h.s of Eq. (15). The resulting approximated version of Eq. (15) gives $\kappa_H^1 \approx \kappa_H^B \approx 1.25\kappa_H^0$ at the dimple (against the computed value $\kappa_H^B = 1.23\kappa_H^0$), and $\kappa^1 \approx \kappa_H^B \approx 0.80\kappa_H^0$ at the rim (computed value: $\kappa_H^B = 0.84\kappa_H^0$, cf. Table 2).

Finally, for what concerns the overall isothermal bending modulus ($\hat{\kappa}_H$), we observe a ≈20% softening with respect to the Born term. In particular, it results $\hat{\kappa}_H = 0.93 \div 0.94\ \kappa_H^0$ at the dimple, and $\hat{\kappa}_H = 0.58 \div 0.59\ \kappa_H^0$ at the rim. We also note that the lowest mesoscopic values of $\hat{\kappa}_H$ are attained at the rim, in correspondence with the peaks of the out-of-plane mean-squared displacement $\langle u_\perp^2 \rangle$ (Fig. 3).

The membrane stiffening associated with area contraction is explained by Eq. (7), which features $\det \mathbf{I}$ at the denominator of the limiting bending energy density W^{bend}, and linear terms in the first fundamental forms g_{ij} at the numerator of the same quantity. It is seen that W^{bend} blows up in the limit $\det \mathbf{I} \to 0$, reproducing compression locking due to progressive material densification. Such a behavior is experimentally observed in soft materials and cellular solids [cf., e.g., Gibson and Ashby (1982)] and is not

captured by planar network models (Discher et al. 1997). Conversely, area expansion ($\det \mathbf{I} > 1$) results in membrane softening. Regarding the explanation of the stiffening effects due to membrane curvature, we refer the reader to the discussion presented in Schmidt and Fraternali (2012). The softening nature of the thermal fluctuations has been illustrated in Sect. 3.

We now compare the present predictions of the shear and bending moduli with analogous results based on the equipartition theorem of statistical mechanics (Lee and Discher 2001; Peliti and Leibler 1985; Kleinert 1986; Gompper and Kroll 1996; Helfrich and Servuss 1984; Helfrich 1985, 1998; Helfrich and Kozlov 1993; Pinnow and Helfrich 2000).

The equipartition approach proposed in Lee and Discher (2001) determines the shear modulus of an isotropic membrane, which fluctuates with prevalent in-plane shear modes (over dilatational modes), through the equation

$$\hat{\mu}_{\mathrm{LD}} \approx k_B T \frac{\log(\Lambda/a)}{2\pi \left\langle u_{\parallel}^2 \right\rangle} \tag{37}$$

where Λ and a represent the maximum and minimum wavelengths characterizing the fluctuations from the mean shape. Eq. (37) accounts for fluctuation effects on the shear rigidity in the infinitesimal elasticity regime. On assuming $\Lambda = \sqrt{A_{\mathrm{tot}}}$ and $a = r_0$ (Marcelli et al. 2005) and setting $\langle u_{\parallel}^2 \rangle$ to the value that we recorded over the rim region, where the total in-plane pressure is almost zero (cf. Table 1), we obtain $\hat{\mu}_{\mathrm{LD}} = 0.89\mu^0$. Let us compare such a prediction with the sum of Born and fluctuation terms of $\hat{\mu}$ computed at the rim through the present theory (sum equal to $1.03\mu^0$, cf. Table 3). The 15% gap between the above estimates of the isotropic shear modulus is explained by shear stiffening due to large deformations, which is accounted for by the present approach (observe that the value of μ^B at the dimple in Table 3 is approximatively 15% higher than μ^0) and is instead neglected in the analysis by Lee and Discher (2001).

For what concerns the bending modulus $\hat{\kappa}_H$ of a fluctuating membrane under zero lateral tension, the approaches proposed in Peliti and Leibler (1985), Kleinert (1986), Gompper and Kroll (1996), Helfrich (1985, 1998), Pinnow and Helfrich (2000) leads to predict the following renormalized value

$$\hat{\kappa}_H = \kappa_H^0 - \frac{\alpha k_B T}{4\pi} \log(\Lambda/a) \tag{38}$$

where α is an amplitude factor, which is equal to 3 according to Peliti and Leibler (1985), Kleinert (1986), Gompper and Kroll (1996); to 1 according to Helfrich (1985); and to -1 according to Helfrich (1998), Pinnow and Helfrich (2000). In the present case, assuming again $\Lambda = \sqrt{A_{\mathrm{tot}}}$ and $a = r_0$, we observe that the difference between $\hat{\kappa}_H$ and κ_H^0 is less than 1%, independently of the value of α (note that $k_B T/(4\pi\kappa_H^0) \approx 3 \times 10^{-4}$ for the model under examination).

The coupled effects of lateral tension and membrane curvature have been examined in Helfrich and Kozlov (1993), where the following formula is proposed for the 'effective bending rigidity'

$$\kappa_H = \kappa_H^0 \left(1 - \frac{3\,\kappa_H^0\, J^2}{2\,\kappa_A^0} \right) \tag{39}$$

Here, κ_A^0 denotes the area compression modulus in the reference (unstretched) configuration, while J denotes the leading curvature of the membrane. On assuming $\kappa_A^0 = \sqrt{3}k/2$ (Schmidt and Fraternali 2012) and setting J to the minimum curvature that we recorded at the rim ($J = H/2 - \sqrt{H^2 - 4K}/2$), we obtain $\kappa_H \approx 0.65\kappa_H^0$ from Eq. (39), which is in good agreement with the value predicted by the present theory ($\hat{\kappa}_H \approx 0.60\kappa_H^0$, cf. Table 2).

5 Concluding remarks

We have presented equilibrium fluctuation formulae for the isothermal elastic moduli of membrane networks of arbitrary shape fluctuating in the 3D Cartesian space. The proposed formulae have been numerically tested with reference to a coarse-grained MD model of the red blood cell membrane (Marcelli et al. 2005; Hale et al. 2009), carrying out an investigation on mesoscopic and macroscopic estimates of the shear and bending moduli of such a model. The numerical analysis has made use of a local maximum-entropy regularization of the geometry of the network [cf. the Appendix and Fraternali et al. (2012)]. A detailed comparison has been established between the present theory and the renormalization approaches presented in (Lee and Discher 2001; Helfrich and Kozlov 1993),

The numerical results obtained for the RBC model have shown regional dependence of the mesoscopic elastic properties on deformation and fluctuation measures. We have detected shear stiffening due to local area contraction and membrane curvature; bending stiffening due to area contraction; shear softening due to thermal fluctuations; and bending softening due to area expansion and thermal fluctuations. Overall, the main conclusions emerging from the numerical study presented in Sect. 4 are the following: (i) the large deformation effects on the RBC membrane rigidity predicted by the present model are not accounted for in standard approaches to the elastic moduli of flexible membranes (cf. Sects. 2, 4.2); (ii) such effects can be analytically estimated by making use of the Eqs. (14), (15) and suitable average strain measures; (iii) the lowest values of the isothermal shear and bending moduli of the RBC membrane are

attained where the in-plane and out-of-plane mean-squared fluctuation displacements reach their peak values, respectively; (iv) positive in-plane pressures 'weaken' the isotropic shear modulus [cf. also Zhou and Joós (1997), Discher et al. (1997)].

The outcomes of the present study can be usefully employed to develop an information-passing multiscale modeling of membrane networks, carrying out finite element simulations at the continuum scale that make use of elastic properties derived from MD simulations. Although the numerical analysis presented in Sect. 4 specifically refers to a triangulated membrane network, we wish to remark that the approach to the elastic moduli of fluctuating networks formulated in Sect. 3 can be conveniently applied to arbitrary networks, provided that the continuum limit of the corresponding discrete potential energy is available.

In closing, we suggest directions for future extensions of the present research. A relevant generalization regards the computation of isothermal elastic moduli in spatial description (or elastic stiffness coefficients), which can be effectively related to experimental measurements [refer, e.g., to Zhou and Joós (2002)]. We indeed plan to apply the present theory to conduct computational simulations of laboratory tests on the RBC mechanics, such as tests based on micropipette aspiration techniques, optical tweezes, fast-phase contrast video microscopy, and/or atomic force microscopy [cf. also Schmidt and Fraternali (2012)]. Another extension might regard the inclusion of initial bending stresses and complex interaction potentials in the proposed equilbrium fluctuation formulae, like, for example, the wormlike chain potential often employed in coarse-grained models of the RBC membrane (Fedosov et al. 2009; Pivkin and Karniadakis 2008; Dao et al. 2006). The use of such potentials could allow us to capture phenomena like strain stiffening of filamentous networks, which have been experimentally observed in biological tissues and cell membranes (refer e.g., to Onck et al. (2005) and references therein). Additional future work also includes the study of phase transitions of membrane networks (Discher et al. 1997), accounting for bending–stretching coupling in the large deformation regime; detailed scale separation studies on the bending modulus of the RBC membrane (Hale et al. 2009), on considering different mesh refinements and model properties; and an extensive validation of the proposed equilibrium fluctuation formulae, to be carried out though a comparative analysis with other available numerical and experimental results, for different types of biomembranes.

Acknowledgments F. F. wishes to acknowledge the great support received by Bernd Schmidt (Institut für Mathematik, Universität Augsburg, Germany), Vincenzo Ciancia (Department of Civil Engineering, University of Salerno, Italy), and Jens Kleinjung (Mathematical Biology Division, National Institute for Medical Research, London, UK) during the course of the present work.

Appendix: Basics of the LME regularization scheme

Given an arbitrary $u \in U$, the LME approximation of the deformation mapping introduced in Sect. 2 is the following

$$f_i(u) \approx \sum_{b=1}^{\tilde{N}} f_{i_b} p_b^*(\mathbf{x}(u)), \tag{40}$$

where $\mathbf{x} = \{x_1, x_2\}$ is the vector of the deformed coordinates in the tangent plane to the current configuration of S (cf. Fraternali et al. (2012), Sect. 3.3); $\tilde{N} \leq N$ is a scalar denoting the number of particles that form the LME regularization set $X^a_{\tilde{N}}$; f_{i_b} are the current deformed positions of the model particles; and p_b^* are the LME shape functions. The latter correspond with the solution of the optimization problem

$$\min_{\{p_1,\ldots,p_{\tilde{N}}\}\in\mathbb{R}^{\tilde{N}}} \left(\beta \sum_{a=1}^{\tilde{N}} p_b \, |\mathbf{x} - \mathbf{x}_b|^2 + \sum_{b=1}^{\tilde{N}} p_b \log p_b \right) \tag{41}$$

subject to:

$$p_b \geq 0, \; b = 1, \ldots, \tilde{N}; \quad \sum_{b=1}^{\tilde{N}} p_b = 1; \quad \sum_{b=1}^{\tilde{N}} p_b \mathbf{x}_b = \mathbf{x} \tag{42}$$

By tuning the value of β in the interval $(0, +\infty)$, the LME scheme suitably balances the maximization of the information entropy corresponding to the given nodal data with the minimization of the total width of the shape functions [local-gobal approximation scheme, cf. Arrojo and Ortiz (2006), Cyron et al. (2009), Fraternali et al. (2012)]. On employing the approximation (40) into (4)–(5), we estimate the instantaneous first and fundamental forms of the fluctuating membrane, accounting for arbitrarily large strains. On the basis of the convergence analysis presented in Fraternali et al. (2012), we choose $\tilde{N}$ so as to include the 10th nearest neighbors of $\mathbf{x}_a$ in the LME regularization set and make use of the following value of β

$$\beta = \frac{125}{\left(\text{diam}(X^a_{\tilde{N}})\right)^2} \tag{43}$$

It has been shown that the above choices of $\tilde{N}$ and β ensure a smooth representation of the RBC membrane, which is particularly able to filter the inherent small scale roughness of the coarse-grained MD model on hand (Fraternali et al. 2012).

References

Arrojo M, Ortiz M (2006) Local maximum-entropy approximation schemes: a seamless bridge between finite elements and meshfree methods. Int J Numer Methods Eng 65:2167–2202

Borelli MES, Kleinert H, Schakel AMJ (1999) Derivative expansion of one-loop effective energy of stiff membranes with tension. Phys Lett A 253:239–246
Cyron CJ, Arrojo M, Ortiz M (2009) Smooth, second-order, non-negative meshfree approximants selected by maximum entropy. Int J Numer Methods Eng 79:1605–1632
Dao M, Li J, Suresh S (2006) Molecularly based analysis of deformation of spectrin network and human erythrocyte. Mater Sci Eng 26:1232–1244
Discher DE, Boal DH, Boey SK (1997) Phase transitions and anisotropic responses of planar triangular nets under large deformation. Phys Rev E 55(4):4762–4772
Fedosov DA, Caswell B, Karniadakis GE (2009) General coarse-grained red blood cell models: I. mechanics. ArXiv e-prints
Fraternali F, Lorenz C, Marcelli G (2012) On the estimation of the curvatures and bending rigidity of membrane networks via a local maximum-entropy approach. J Comput Phys 231:528–540
Gibson L, Ashby M (1982) The mechanics of three-dimensional cellular materials. Proc R Soc Lond A Mat 382(1782):43–59
Gompper G, Kroll D (1996) Random surface discretization and the renormalization of the bending rigidity. J Phys I Fr 6:1305–1320
Hale J, Marcelli G, Parker K, Winlowe C, Petrov G (2009) Red blood cell thermal fluctuations: comparison between experiment and molecular dynamics simulations. Soft Matter 5:3603–3606
Hartmann D (2010) A multiscale model for red blood cell mechanics. Biomech Model Mechanobiol 9:1–17
Helfrich W (1985) Effect of thermal undulations on the rigidity of fluid membranes and interfaces. J Phys 46:1263–1268
Helfrich W (1998) Stiffening of fluid membranes and entropy loss of membrane closure: two effects of thermal undulations. Eur Phys J B 1:481–489
Helfrich W, Kozlov MM (1993) Bending tensions and the bending rigidity of fluid membranes. J Phys II Fr 3:287–292
Helfrich W, Servuss R (1984) Untlulations, steric interactian and cohesion of fldd untlulations, steric interaction and cohesion of fluid membranes. Nuovo Cimento 1:137–151
Hess S, Kröger M, Hoover W (1997) Shear modulus of fluids and solids. Phys A 239
Holzapfel GA (2000) Nonlinear solid mechanics, a continuum approach for engineering. Wiley, Chichester
Kleinert H (1986) Thermal softening of curvature elasticity in membranes. Phys Lett A 114:263–268
Kohyama T (2009) Simulations of flexible membranes uding a coarse-grained particle-based model with spontaneous curvature variables. Phys A 388:3334–3344
Kühnel W (2002) Differential geometry, curves-surfaces-manifolds. American Mathematical Society, Providence, RI
Lee J, Discher D (2001) Deformation-enhanced fluctuations in the red cell skeleton with theoretical relations to elasticity, connectivity, and spectrin unfolding. Biophys J 81:3178–3192
Lipowsky R, Girardet M (1990) Shape fluctuations of polymerized or solidlike membranes. Phys Rev Lett 65(23):2893–2896
Lutsko J (1989) Generalized expressions for the calculation of the elastic constants by computer simulation. J Appl Phys 8:2991–2997
Marcelli G, Parker H, Winlove P (2005) Thermal fluctuations of red blood cell membrane via a constant-area particle-dynamics model. Biophys J 89:2473–2480
Mecke KR (1995) Bending rigidity of fluctuating membranes. Z Phys B Condens Mater 97:379–387
Müller M, Katsov K, Schick M (2006) Biological and syntetic membranes: what can be learned from a coarse-grained description?. Phys Rep 434:113–176
Munkres J (1984) Elements of algebraic topology. Addison-Wesley, Menlo Park, CA
Naghdi PM (1972) The theory of shells and plates. In: Flügge's S (ed) Handbuch der Physik, Vol. VIa/2, C. Trusdell Ed.. Springer, Berlin, pp 425–640
Nelson D, Piran T, Weinberg S, (eds) (2004) Statistical mechanics of membranes and surfaces, 2nd edn. World Scientific, Singapore
Ogden RW (1984) Non-linear elastic deformations. Dover, Mineola
Onck P, Koeman T, van Dillen T, van der Glessen E (2005) Alternative explanation of stiffening in cross-linked semiflexible networks. Phys Rev Lett 95
Peliti L, Leibler S (1985) Effects of thermal fluctuations on systems with small surface tensionl fluctuations on systems with small surface tension. Phys Rev Lett 54:1690–1693
Pinnow H, Helfrich W (2000) Effect of thermal undulations on the bending elasticity and spontaneous curvature of fluid membranes. Eur Phys J E 3:149–157
Pivkin I, Karniadakis G (2008) Accurate coarse-grained modeling of red blood cells. Phys Rev Lett 101
Ray J, Rahman A (1984) Statistical ensembles and molecular dynamics studies of anisotropic solids. J Chem Phys 80(9):4423–4428
Schmidt B (2006) A derivation of continuum nonlinear plate theory from atomistic models. SIAM Multiscale Model Simul 5:664–694
Schmidt B (2008) On the passage from atomic to continuum theory for thin films. Arch Ration Mech Anal 190:1–55
Schmidt B, Fraternali F (2012) Universal formulae for the limiting elastic energy of static membrane networks. J Mech Phys Solids 60:172–180
Schöffel P, Möser MH (2001) Elastic constants of quantum solids by path integral simulations. Phys Rev B 63(224108):1–9
Seung H, Nelson D (1988) Defects in flexible membranes with crystalline order. Phys Rev A 38:1005–1018
Smith W, Forester T (1999) The dl_poly_2 molecular simulation package. http://www.cse.clrc.ac.uk/msi/software/DL_POLY
Squire D, Holt A, Hoover W (1969) Isothermal elastic constants for argon. Theory and monte carlo calculations. Physica 42:388–397
Tu ZC, Ou-Yang ZC (2008) Elastic theory of low-dimensionale continua and its application in bio- and nano-structures. J Comput Theor Nanosci 5:422–448
Yoshimoto K, Papakonstantopoulos G, Lutsko J, de Pablo J (2005) Statistical calculation of the elastic moduli for atomistic models. Phys Rev B 71(181108):1–6
Zhou Z, Joós B (1996) Stability criteria for homogeneously stressed materials and the calculation of elastic constants. Phys Rev B 54(6):3841–3850
Zhou Z, Joós B (1997) Mechanisms of membrane rupture: from cracks to pores. Phys Rev B 56:2997–3009
Zhou Z, Joós B (1999) Convergence issues in molecular dynamics simulations of highly entropic materials. Model Simul Mater Sci Eng 7:383–395
Zhou Z, Joós B (2002) Fluctuation formulas for the elastic constants of an arbitrary system. Phys Rev B 66